

OMNIINFER: SYSTEM-WIDE ACCELERATION TECHNIQUES FOR OPTIMIZING LLM SERVING THROUGHPUT AND LATENCY

Jun Wang¹ Yunxiang Yao¹ Wenwei Kuang¹ Runze Mao¹ Zhenhao Sun¹ Zhuang Tao¹ Ziyang Zhang¹
Dengyu Li¹ Jiajun Chen¹ Zhili Wang¹ Kai Cui¹ Congzhi Cai¹ Longwen Lan¹ Ken Zhang^{*1}

ABSTRACT

Large Language Models drive a wide range of modern AI applications but impose substantial challenges on large-scale serving systems due to intensive computation, strict latency constraints, and throughput bottlenecks. We introduce OmniInfer, a unified system-level acceleration framework designed to maximize end-to-end serving efficiency through fine-grained optimization of expert placement, cache compression, and scheduling. OmniInfer integrates three complementary components: OmniPlacement for load-aware Mixture-of-Experts scheduling, OmniAttn for sparse attention acceleration, and OmniProxy for disaggregation-aware request scheduling. Built atop vLLM, OmniInfer delivers system-wide performance gains through adaptive resource disaggregation, efficient sparsity exploitation, and global coordination across prefill and decode phases. Evaluated on DeepSeek-R1 within a 10-node Ascend 910C cluster, OmniInfer achieves 616 QPM, where the unified framework reduces TPOT by 36%, and the superimposition of OmniProxy further slashes TTFT by 38%. The project is open-sourced at <https://gitee.com/omniai/omniainfer>.

1 INTRODUCTION

Large Language Models (LLMs) like DeepSeek (Guo et al., 2025a), Qwen (Yang et al., 2025), Kimi (Team et al., 2025) and GPT (Agarwal et al., 2025) have rapidly become the foundation of modern AI applications, powering chatbots (Achiam et al., 2023), tool use (Schick et al., 2023), search (ZillizTech, 2025), and multimodal assistants (Sharon & Brichtova, 2025). However, their deployment at scale remains challenging due to enormous computational demands and stringent service-level objectives (SLOs), such as low time-to-first-token (TTFT) and high query-per-minute (QPM) throughput. To sustain practical serving, systems must not only maximize hardware utilization but also optimize scheduling across diverse and dynamic workloads.

Existing LLM serving systems have made substantial progress in improving inference efficiency, leveraging techniques such as operator fusion (Zuo et al., 2025), continuous batching (Kwon et al., 2023), and KV-cache reuse (Zheng et al., 2024). However, most of these systems assume homogeneous clusters and monolithic execution, where the prefill and decode stages are tightly coupled. This design overlooks the distinct computational and memory characteristics of the two phases: the prefill stage is compute-intensive, domi-

nated by large matrix multiplications, whereas the decode stage is memory- and communication-bound, constrained by KV-cache accesses and sequential token generation (Patel et al., 2024; Zhong et al., 2024). Recent variants such as chunked prefill (Agrawal et al., 2024) attempt to reduce TTFT under continuous batching, but fundamentally shift rather than eliminate prefill-decode interference, and thus cannot fully resolve the inherent contention between the two stages. Treating the two phases uniformly not only results in inefficient hardware utilization but also exacerbates head-of-line (HOL) blocking under dynamic workloads (Zhou et al., 2024; Pan & Li, 2025).

To mitigate these inefficiencies, recent work has explored prefill-decode (PD) disaggregation (Zhong et al., 2024; Patel et al., 2024), which separates prefill and decode across different hardware resources. This approach enables finer-grained scheduling, better load balancing, and new opportunities for parallelization. Nonetheless, current PD disaggregation systems remain limited: many assume high-speed interconnects that are not universally available, while others lack global scheduling policies capable of adapting to fluctuating workloads. Consequently, while PD disaggregation represents an important step forward, it alone does not fully address the broader bottlenecks in modern LLM serving.

Beyond PD disaggregation, existing serving frameworks continue to face two fundamental challenges. First, *sparse computing*, arising from mixture-of-experts (MoE) models and sparse attention mechanisms, offers theoretical effi-

^{*}Project lead ¹Theory Lab, Central Research Institute, 2012 Labs, Huawei Technologies Co., Ltd. Correspondence to: Jun Wang <wang.jun7@huawei.com>, Ken Zhang <ken.zhang1@huawei.com>.

ciency gains but often introduces load imbalance and hardware under-utilization in practice (Liu et al., 2024b). Second, while several heuristic and black-box optimization (Fu et al., 2024; Singh et al., 2025) approaches have been proposed for *smart scheduling*, they generally overlook the distinct characteristics of the prefill and decode phases in LLM inference. As LLMs scale toward larger and multimodal forms, these limitations increasingly constrain throughput, latency, and cost efficiency.

In this paper, we present OmniInfer, a unified suite of acceleration techniques designed to achieve efficient large-scale LLM serving. OmniInfer holistically tackles both sparse computing and smart scheduling, enabling end-to-end optimizations across the serving stack. Our design philosophy is to decouple major serving bottlenecks into specialized modules, while preserving a unified interface for deployment in production systems.

Concretely, OmniInfer makes three core contributions that are modular, orthogonal and synergize with each other:

- **OmniPlacement**: a load-aware MoE expert scheduling mechanism that improves efficiency in MoE inference.
- **OmniAttn**: optimized sparse attention that accelerates long-context inference while preserving model quality.
- **OmniProxy**: a scheduling proxy that coordinates prefill and decode phases using disaggregation-aware strategies to optimize throughput and latency.

We implement OmniInfer on top of a state-of-the-art serving framework vLLM (Kwon et al., 2023) and conduct extensive experiments with popular open-source LLMs. Our evaluation on a 10-node Ascend 910C cluster shows that OmniInfer achieves up to 616 QPM, where the unified framework reduces TPOT by up to 36%, and the superimposed OmniProxy further reduces TTFT by up to 38%. These results establish OmniInfer as a practical, scalable, and cost-efficient solution for next-generation LLM serving.

2 BACKGROUND AND RELATED WORK

LLM Serving Serving large language models poses unique challenges due to the heterogeneous nature of their inference workloads. The prefill and decode phases exhibit distinct computational characteristics—prefill is compute-intensive, whereas decode is dominated by memory and communication bottlenecks. Treating these stages uniformly leads to resource imbalance and head-of-line blocking when serving dynamic workload. To overcome these limitations, emerging research has embraced disaggregated serving, which decouples prefill and decode execution across heterogeneous resources. Systems such as SplitWise (Patel et al., 2024), DistServe (Zhong et al., 2024), and DéjàVu (Strati

et al., 2024) demonstrate that such separation alleviates stage interference and improves both TTFT and throughput. Building on this idea, Mooncake (Qin et al., 2025) and PD-Serve (Jin et al., 2024) incorporate advanced KV-cache management and fine-grained resource scheduling, while EPD (Singh et al., 2025) extends the paradigm to multimodal settings by further disaggregating the encoding stage, thereby enabling enhanced system efficiency.

Sparse Computing The quadratic complexity of self-attention in long-context LLMs has motivated extensive research into sparse computation for efficient inference. One direction focuses on KV cache sparsification, where redundant tokens are selectively pruned to reduce the memory footprint. Techniques such as H2O (Zhang et al., 2023) and SnapKV (Li et al., 2024) exemplify this approach by identifying and retaining a subset of recent and contextually critical tokens. Another direction modifies the attention topology itself. Building on the “attention sink” phenomenon, methods like DuoAttention (Xiao et al., 2025) design fixed sparse patterns that combine local sliding windows with persistent attention to global anchors, thereby reducing computational overhead while maintaining contextual coherence. Departing from these training-dependent paradigms, OmniAttn embraces an inference-driven perspective: instead of learning sparsity through gradient-based optimization, it exploits search-based compression to automatically discover efficient attention patterns. This decouples sparsity design from model training and enables flexible deployment across heterogeneous serving environments.

Beyond attention sparsity, serving Mixture-of-Experts (MoE) models (Liu et al., 2024b; Fedus et al., 2022) introduces another dimension of sparsity—expert sparsity—arising from token-level dynamic routing. Such irregular activation often causes severe load imbalance and hardware underutilization. While systems like DeepSpeed-MoE (Rajbhandari et al., 2022) and Tutel (Hwang et al., 2023) optimize low-level kernels, they still rely on static expert placement or capacity-based token dropping. Architectural approaches such as expert-choice routing (Zhou et al., 2022) mitigate imbalance at the model level but lack runtime adaptability. More recent adaptive methods (Yue et al., 2025; Guo et al., 2025b) adjust expert activation dynamically based on context, yet they remain reactive rather than anticipatory. In contrast, OmniPlacement provides a proactive, closed-loop control mechanism that continuously monitors expert utilization and performs lightweight, non-blocking weight migration in response to evolving workloads. This allows for balanced and efficient serving of MoE models without architectural modification, offering a generalizable systems-level solution to expert imbalance.

LLM Scheduling Scheduling in LLM serving faces two fundamental challenges: long shared prompts and var-

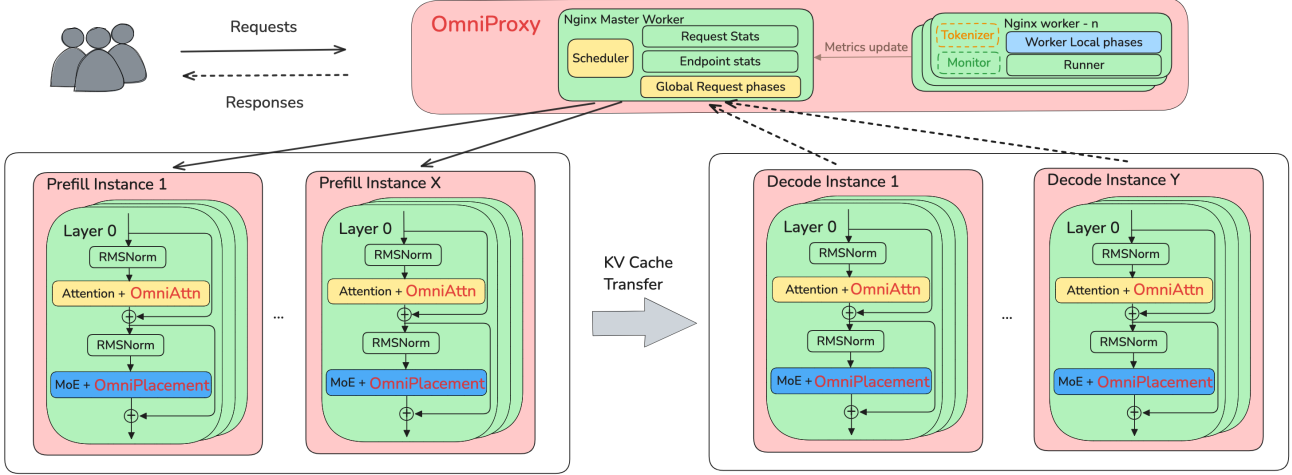


Figure 1. Structure of OmniInfer system under PD-disaggregated serving.

ied prompt lengths. For the first, requests with long or shared prompts necessitate KV-cache-aware prefill scheduling, since cache locality and reuse can significantly reduce redundant computation. Recent systems such as Preble (Srivatsa et al., 2025), MemServe (Hu et al., 2024), and SGLang (Zheng et al., 2024) adopt radix-tree-based approaches to efficiently identify and exploit KV-cache overlap. For the second, heterogeneous prompt lengths introduce execution bubbles in both prefill and decode stages, degrading throughput and latency. To mitigate this, works such as EfficientLLM (Fu et al., 2024) employ Shortest-Job-First (SJF) principles to align with service-level objectives (SLOs), while others (Fu et al., 2024; Stojkovic et al., 2025) leverage small language models to predict generation lengths or rank requests, providing more accurate workload estimation or ranking.

From a scheduling perspective, many approaches rely on heuristic rules, e.g., SJF-based policies (Fu et al., 2024) or KV-aware heuristics (Srivatsa et al., 2025), whereas systems such as DistServe (Zhong et al., 2024) and EPD (Singh et al., 2025) adopt black-box optimization solvers for decision-making. However, prior efforts typically focus on either shared prompts or varied prompt lengths in isolation. In contrast, our proposed OmniProxy addresses both issues simultaneously. By leveraging endogenous system metrics, OmniProxy achieves more precise scheduling across diverse and dynamic serving scenarios.

3 SYSTEM OVERVIEW

OmniInfer is designed as a *modular acceleration suite* for large-scale LLM serving. Our core design principle is to identify key performance bottlenecks and provide *targeted and pluggable* optimizations that can be easily integrated into mainstream inference frameworks such as vLLM and

SGLang. Instead of tightly coupling with a specific runtime, OmniInfer focuses on three critical acceleration points: MoE expert placement, sparse attention, and global request-level scheduling.

Architecture. OmniInfer consists of three lightweight components (Figure 1): (1) OmniPlacement, a load-aware expert scheduler for balancing sparse MoE computation; (2) OmniAttn, efficient sparse attention kernels to reduce memory and compute overhead; and (3) OmniProxy, a disaggregation-aware scheduling proxy coordinating prefill and decode execution. Requests first enter OmniProxy, which classifies and dispatches them to specialized prefill or decode workers. OmniPlacement and OmniAttn accelerate execution at the model layers, and OmniProxy aggregates results to reduce TTFT and improve QPM.

4 SPARSE COMPUTING IN OMNIINFER

In large-scale LLM inference, sparse computation introduces unique performance bottlenecks: uneven expert activation leads to severe load imbalance in MoE models, while dense attention incurs excessive KV-cache and compute overhead. To address these issues, OmniInfer integrates two complementary acceleration modules—OmniPlacement for adaptive expert scheduling and OmniAttn for attention sparsification—jointly improving both throughput and

4.1 OmniPlacement: Expert Scheduling for MoE

Mixture-of-Experts (MoE) inference frequently encounters severe load imbalance, characterized by a subset of “hot” experts receiving a disproportionate share of activations. This skew creates computational bottlenecks on specific devices, thereby increasing end-to-end latency and throttling overall system throughput.

To mitigate this, we propose OmniPlacement, a dynamic, near real-time expert placement algorithm. OmniPlacement exploits expert redundancy and a lightweight scheduling mechanism to rapidly adapt to fluctuating workload patterns. Our approach is designed to maintain consistently balanced expert utilization, thereby substantially enhancing MoE inference performance.

Problem Formulation We consider an MoE model comprising L layers, with E experts per layer, deployed across a cluster of R devices. The expert placement is represented by a binary tensor $P \in \{0, 1\}^{L \times R \times E}$, where $P_{l,r,e} = 1$ indicates that expert e of layer l is hosted on device r .

Constraints. The placement is subject to two primary constraints. First, to ensure model integrity, every expert must be available on at least one device:

$$\sum_{r=0}^{R-1} P_{l,r,e} \geq 1, \quad \forall l, e. \quad (1)$$

Second, we impose a capacity constraint to manage memory usage. Each device allocates a fixed budget of s_l expert “slots” for layer l . The parameter s_l , termed the redundancy factor, dictates the replication level. This constraint is expressed as:

$$\sum_{e=0}^{E-1} P_{l,r,e} \leq s_l, \quad \forall l, r. \quad (2)$$

A larger s_l increases the redundancy budget ($s_l R - E$ total replicas), allowing “hot” experts to be replicated across multiple devices to distribute load, albeit at the cost of higher memory consumption.

Objective. Our goal is to minimize load imbalance. To formalize this, we define the expert load matrix $D \in \mathbb{R}_{\geq 0}^{L \times E}$. Each entry $D_{l,e}$ represents the estimated computational load of expert e in layer l . This value is derived from historical activation statistics (e.g., via a sliding window average) to capture recent workload trends while filtering out transient noise. Given the placement P and load matrix D , the total load on device r for layer l is the aggregate load of its hosted experts:

$$R_r(l, P, D) = \sum_{e=0}^{E-1} P_{l,r,e} \cdot D_{l,e}. \quad (3)$$

We define the *load imbalance ratio* $B(l, P, D)$ as the ratio of the peak device load to the average device load:

$$B(l, P, D) = \frac{\max_i R_i(l, P, D)}{\frac{1}{R} \sum_j R_j(l, P, D)}. \quad (4)$$

A ratio of 1.0 indicates perfect balance. Our objective is to find a placement P that minimizes this ratio subject to the aforementioned constraints.

OmniPlacement Algorithms To achieve the goals, our expert management strategy, OmniPlacement, consists of two core components. First, a static placement algorithm (Algorithm 1) generates an optimal initial layout by strategically allocating redundant experts to balance the initial load. Second, a dynamic scheduler (Algorithm 2) continuously monitors the system and performs online adjustments to adapt to shifting workloads. Both algorithms are presented below to highlight their primary logic.

Algorithm 1 Static Expert Placement

Require: Load matrix D , number of layers L , number of devices R , total redundancy budget M

Ensure: Optimal static placement P^*

```

1:  $s \leftarrow \text{AllocateBudgetByImbalance}(D, L, M)$ 
2: for  $l = 0$  to  $L - 1$  do
3:    $P_l^{\text{best}} \leftarrow \text{null}, B_{\min} \leftarrow \infty$ 
4:   for  $k = 0$  to  $s_l$  do
5:      $C \leftarrow \text{DetermineReplicas}(D_l, k, R)$ 
6:      $P^k \leftarrow \text{GeneratePlacement}(C, D_l, R)$ 
7:      $B_k \leftarrow \text{CalculateImbalance}(P^k, D_l)$ 
8:     if  $B_k < B_{\min}$  then
9:        $P_l^{\text{best}} \leftarrow P^k$ 
10:       $B_{\min} \leftarrow B_k$ 
11:     end if
12:   end for
13:    $P_l^* \leftarrow P_l^{\text{best}}$ 
14: end for
15: return  $P^*$ 

```

The OmniPlacement process begins with the Static Expert Placement algorithm, detailed in Algorithm 1. Its purpose is to compute an optimal initial expert layout based on a given activation distribution. The process starts by intelligently distributing the total memory budget; the `AllocateBudgetByImbalance` function (line 1) analyzes historical activation data D to assign a larger portion of the total redundancy budget M to layers exhibiting higher load imbalance, ensuring resources are prioritized where they are most needed. Next, for each layer, the algorithm seeks the best placement within its allocated budget s_l . It iterates through possible redundancy levels (line 4) and, for each level, first calls `DetermineReplicas` (line 5). This function employs a heap-based greedy strategy to identify the most frequently activated (“hot”) experts and determines how many replicas of each are needed. With the replica counts decided, the `GeneratePlacement` function (line 6) then maps these expert instances to physical devices. This is a two-step process: an initial greedy placement assigns experts to the least-loaded devices, followed by a topology-aware remapping that adjusts the layout to minimize inter-device communication costs. By simulating and evaluating the imbalance for each potential configuration (lines 7-10), the algorithm selects the placement P^* that achieves the minimum load imbalance, ensuring the system starts in a highly balanced state.

Once the system is running, the Dynamic Expert Scheduler (Algorithm 2) takes over to perform continuous, on-line optimization. The scheduler monitors real-time expert activations and updates a sliding window of workload data (line 4). If the current load imbalance B_{current} surpasses a trigger threshold B_{trigger} (line 6), it initiates a rebalancing procedure. To make proactive decisions, it first calls `PredictFutureActivations` (line 7), a function that analyzes recent activation trends to forecast the workload D_{pred} for the upcoming time interval. This predictive approach allows the system to adapt to shifting patterns before they become critical bottlenecks. Using this predicted workload, a new candidate placement P_{cand} is generated by invoking the static placement algorithm (line 8). To prevent system instability from frequent, minor adjustments, this new placement is only adopted if its simulated imbalance B_{sim} shows a significant improvement over the current state, exceeding a predefined margin Δ (line 11). If the change is accepted, the `ExecuteMigration` function is called (line 11) to apply the new layout. In essence, this function orchestrates the physical migration of expert weights, ensuring a seamless transition with minimal impact on ongoing inference tasks.

Algorithm 2 Dynamic Expert Scheduler

Require: Initial placement P_{init} , imbalance trigger threshold B_{trigger} , improvement margin Δ , memory budget M

Ensure: Continuously updated placement P_{current}

```

1:  $P_{\text{current}} \leftarrow P_{\text{init}}$ 
2:  $D \leftarrow \text{InitializeActivationWindow}()$ 
3: while system is running do
4:    $D \leftarrow \text{UpdateActivationWindow}()$ 
5:    $B_{\text{current}} \leftarrow \text{CalculateImbalance}(P_{\text{current}}, D)$ 
6:   if  $B_{\text{current}} > B_{\text{trigger}}$  then
7:      $D_{\text{pred}} \leftarrow \text{PredictFutureActivations}(D)$ 
8:      $P_{\text{cand}} \leftarrow \text{StaticExpertPlacement}(D_{\text{pred}}, L, R, M)$ 
9:      $B_{\text{sim}} \leftarrow \text{CalculateImbalance}(P_{\text{cand}}, D_{\text{pred}})$ 
10:    if  $B_{\text{sim}} < B_{\text{current}} - \Delta$  then
11:      ExecuteMigration( $P_{\text{current}}, P_{\text{cand}}$ )
12:       $P_{\text{current}} \leftarrow P_{\text{cand}}$ 
13:    end if
14:  end if
15:  Wait for next scheduling interval
16: end while
    
```

Layer-Wise Redundant Deployment OmniPlacement adaptively allocates replicas based on the imbalance ratio $B(l, P, D)$. Layers exhibiting high imbalance receive additional replicas for their “hot” experts, while stable layers remain compact. This heterogeneous resource distribution directs memory overhead specifically toward bottleneck layers, offering superior robustness against load spikes compared to uniform redundancy schemes.

Near Real-Time Scheduling and Monitoring To facilitate dynamic adaptation, OmniPlacement employs an asynchronous monitoring component running on a separate com-

putation stream. This component tracks expert activations in real-time without blocking the main inference process. The load $D_{l,e}$ is computed via a weighted moving average, effectively filtering transient noise. This data drives the imbalance calculations in Equation (4), enabling the scheduler to rapidly converge to near-optimal configurations.

Pipelined Expert Weight and Placement Updates We implement a sophisticated pipeline to decouple weight migration from inference. While inference proceeds on the main stream, expert weights are transferred in the background using a dedicated communication stream, leveraging primitives such as Huawei’s Collective Communication Library (HCCL) for low-latency transport. The update concludes with an atomic switch to the new configuration once migration is complete. This pipelined approach enables seamless updates, ensuring that migration overhead has a negligible impact on inference latency.

4.2 OmniAttn: Sparse Attention Acceleration

The attention patterns of large language models (LLMs) are often inherently sparse: many attention heads consistently focus on only a small subset of key tokens, while the remaining positions contribute marginally to the output. Recent empirical studies, such as Streaming LLM (Xiao et al., 2024) and Duo Attention (Xiao et al., 2025), reveal that attention is typically concentrated on the earliest tokens (i.e., *attention sink*) and the most recent tokens (i.e., *recent*), whereas intermediate tokens receive near-zero attention scores. This observation enables a principled reduction of KV-cache size and attention computation cost without significantly compromising generation quality. Capitalizing on this, we propose OmniAttn, a KV cache compression algorithm that employs a layer-wise pruning pattern and a fast pattern search method based on an evolutionary algorithm.

Problem Formulation. Given a query matrix $Q \in \mathbb{R}^{K \times d}$, and key and value matrices $K, V \in \mathbb{R}^{M \times d}$, we aim to identify a small subset of token indices $\mathcal{M} \subseteq \{1, 2, \dots, M\}$ with size $N = |\mathcal{M}| \ll M$.

Let $K_{\mathcal{M}} \in \mathbb{R}^{N \times d}$ and $V_{\mathcal{M}} \in \mathbb{R}^{N \times d}$ be the matrices formed by selecting the rows from K and V corresponding to the indices in \mathcal{M} . The goal is to find an \mathcal{M} such that the following approximation holds:

$$\text{softmax} \left(\frac{QK_{\mathcal{M}}^{\top}}{\sqrt{d}} \right) V_{\mathcal{M}} \approx \text{softmax} \left(\frac{QK^{\top}}{\sqrt{d}} \right) V. \quad (5)$$

In OmniAttn, \mathcal{M} is constructed by selecting tokens from the *attention sink region* and the *recent region*, i.e.,

$$\mathcal{M} := \{1, 2, \dots, N_{\text{sink}}\} \cup \{M - N_{\text{recent}} + 1, \dots, M\}, \quad (6)$$

where N_{sink} and N_{recent} are hyperparameters controlling compression granularity. In contrast to methods such as

StreamingLLM (Xiao et al., 2024), we apply pattern search for layer-wise attention compression as described in the following.

Layer-wise Compression. While prior sparse attention methods typically apply compression at the attention head level, this introduces imbalanced head effects under tensor parallelism (TP), where compressed heads must wait for the slowest uncompressed head to complete. To address this, OmniAttn performs compression at the layer level, treating each Transformer layer as the minimal compression unit. This design eliminates synchronization delays under TP and is also compatible with Multi-Latent Attention (MLA)-style architectures (Liu et al., 2024a; Ji et al., 2025). However, applying a single pruning strategy to all heads within a layer presents a greater challenge in maintaining model accuracy. To address this, we introduce a fast pattern search algorithm that efficiently and thoroughly explores the configuration space at an inference-only cost.

Pattern Search. Unlike prior works like DuoAttention (Xiao et al., 2025) that rely on end-to-end training to learn pruning patterns – a process that is computationally and memory intensive due to the need for gradient computation – OmniAttn adopts a search-based strategy. We leverage an evolutionary algorithm to discover high-performance layer-wise compression patterns at an inference-only cost, avoiding any training process.

Specifically, we employ a genetic algorithm to find a compression pattern that minimizes inference latency while adhering to a specified accuracy budget. Each candidate pattern is represented as a binary vector $p \in \{0, 1\}^L$, where each element indicates whether the corresponding layer is compressed. The search proceeds as follows:

1. Initialization: A population of candidate patterns is generated randomly.
2. Evaluation: Each pattern is used to configure the model’s KV cache, and the model’s accuracy is evaluated on a held-out dataset. This accuracy score serves as the pattern’s fitness.
3. Evolution: The population undergoes selection, crossover (evolution), and mutation over multiple generations, favoring patterns with higher fitness scores.

The search terminates after a fixed number of generations or upon early stopping if a pattern exceeds the target accuracy threshold τ . This process can be formalized as the following optimization problem:

$$\min_p \text{Latency}(p) \quad \text{s.t.} \quad \text{Acc}(p) \geq \tau, \quad (7)$$

where p is the layer-wise compression pattern.

5 SMART SCHEDULING IN OMNIINFER

Modern LLM inference pipelines face significant performance degradation when scheduling is handled locally and reactively, often leading to suboptimal batching, cache underutilization, and tail latency amplification. In this section, we introduce OmniProxy—a global, disaggregation-aware scheduling layer that leverages performance prediction, inference periodicity, and Automatic Prefix Cache (APC)-aware cache coordination to jointly optimize prefill and decode phases under dynamic workloads.

5.1 OmniProxy: Global PD Adaptive Scheduler

To make globally optimal scheduling decisions under heterogeneous and dynamic workloads, OmniProxy acts as the central scheduling layer that coordinates both the prefill and decode phases. It integrates system-level lifecycle management with adaptive scheduling algorithms, enabling fine-grained request reordering, batching, and load distribution while minimizing tail latency.

System Framework. OmniProxy is built on top of the high-performance network service framework *Nginx*, and extends it with three core capabilities:

Unified Request Lifecycle. A unified request lifecycle management layer is introduced to coordinate execution across the Prefill and Decode stages. It enables flexible state transitions, fine-grained timing control, and cache-aware routing. The full lifecycle comprises eight phases: tokenize, APC matching, Prefill waiting, Prefill scheduled, Prefill running, Decode waiting, Decode scheduled, and Decode running.

Real-Time Performance Metrics Collecting. OmniProxy continuously gathers both request-level signals (e.g., prompt length, prefix-match score, TPOT, TTFT) and instance-level metrics (e.g., queue length, batch execution time, throughput). These real-time measurements form the basis for predictive and feedback-driven scheduling decisions.

Deferred Submission and Resorting. Unlike *Nginx*, which schedules and dispatches requests immediately upon arrival, OmniProxy defers submission to the backend and performs dynamic resorting. By incorporating the predicted upstream batch cycle into the scheduling process, the system ensures that deferral introduces minimal impact on TTFT. This postponed submission provides additional flexibility to form more coherent request groups and achieve more balanced load balancing across the Prefill and Decode stages.

Omni Adaptive Scheduling (OAS) Algorithm. Built upon this system framework, OmniProxy proposes an Omni Adaptive Scheduling (OAS) algorithm that uses both request-level and instance-level signals to achieve globally coordinated scheduling:

Prefill Side: Cache-Informed Load-Balanced Scheduling. OmniProxy integrates with the inference engine’s Automatic Prefix Cache (APC) mechanism (vLLM Contributors, 2025). For an incoming request i , OmniProxy evaluates each candidate prefill node using the scheduling score,

$$\pi_P(i) = \text{Match}_P(i) - \alpha \rho_P, \quad (8)$$

where $\text{Match}_P(i)$ denotes the prefix match score obtained via radix-tree lookup, and ρ_P represents the instantaneous load of the prefill node, i.e., the number of running requests and tokens. The coefficient α controls the trade-off between cache locality and load balancing. This formulation enables OmniProxy to maximize cache reuse while preventing load concentration on any single node.

Decode Side: Processing-Time–Oriented Scheduling. For the decode stage, OmniProxy estimates the effective workload of request i as

$$\ell_i = T_i^{\text{prompt}} + T_i^{\text{max}}, \quad (9)$$

where T_i^{prompt} and T_i^{max} denote prompt length and max tokens if provided. Requests are then scheduled according to a Longest-Processing-Time-First (LPT) policy to minimize execution gaps and improve throughput.

6 EVALUATION

We conduct a comprehensive experimental evaluation to assess the efficiency, scalability, and accuracy of OmniInfer under realistic large-scale inference workloads. Our experiments are designed to answer three key questions: (i) *How well does OmniInfer scale with different prefill and decode configurations?* (ii) *How much does each acceleration component contribute to end-to-end performance?* and (iii) *Does the use of sparse attention affect model accuracy?* All experiments are conducted on realistic hardware configurations and widely used LLM models, ensuring the results reflect practical deployment conditions.

6.1 Experimental Setup

Datasets. We construct a synthetic dataset derived from large-scale online novel corpora to emulate real-world long-context generation scenarios. The dataset features variable-length input and output sequences, with an average input length of approximately 3,500 tokens and an average output length of about 1,000 tokens. The combined sequence length (input plus output) is capped below 16K tokens. Both input and output length distributions exhibit a pronounced long-tail pattern, reflecting the heterogeneous nature of real LLM serving workloads.

Benchmarking. To impose sustained and controllable system load, we design a customized benchmarking script that

Table 1. Scaling experiment results under different xPyD configurations.

xPyD	Batch Size/die	QPM (r/s)	TTFT (s)	TPOT (ms)
4P8-1D32	24	472	2.598	38
5P8-1D32	30	500	1.548	41
5P8-1D32	32	520	1.983	42
6P8-1D32	40	524	1.282	48
6P8-1D32	44	552	1.630	50
6P8-1D32	46	549	1.537	51
6P8-1D32	48	572	2.196	52
8P8-1D64	24	481	2.822	37

maintains a fixed concurrency level throughout the evaluation. Specifically, if n requests are completed during a given time interval, the benchmarking system immediately injects n new requests to keep the number of in-flight requests constant. This ensures that the serving system operates under steady-state pressure, enabling a fair comparison of scheduling strategies and resource utilization efficiency.

Implementation Details. All experiments are conducted on Ascend 910C NPUs using DeepSeek-R1 models with INT8 quantization. We evaluate the performance of OmniInfer under different prefill and decode configurations. For the prefill (P) stage, each Ascend 910C node employs 16-way tensor parallelism.¹ We use the P8 configuration, meaning that one Ascend 910C node hosts a single DeepSeek-R1 model with TP16. For the decode (D) stage, we evaluate two configurations: D32 and D64, corresponding to 64-way and 128-way data parallelism, respectively. These settings involve four-node and eight-node Ascend 910C nodes per model. The batch size reported in our experiments refers to the per-die batch size. The total system-wide batch size is computed as: $\text{system-level batch size} = \text{per-die batch size} \times \# \text{NPU nodes} \times 8 \times 2$. For example, under the 4P8-1D32 configuration with a per-die batch size of 24, the system consists of four prefill nodes, each hosting a single DeepSeek-R1 model with TP16, and one decode node composed of four Ascend 910C nodes serving a DeepSeek-R1 model with DP64. The total concurrency for this system is 1536.

6.2 Experimental Results

Scaling Experiments To investigate the impact of system configuration on serving efficiency, we conduct scaling experiments by varying the ratio of prefill and decode nodes (xPyD) and the batch size. We measure throughput and latency metrics, including Queries Per Minute (QPM), Time-To-First-Token (TTFT), and Time-Per-Output-Token (TPOT). The results are summarized in Table 1. From the results, several observations can be made.

¹Each Ascend 910C device consists of two dies, resulting in 16 dies per node.

Table 2. End-to-End performance study of OmniInfer. We report tail-latency, throughput, and efficiency metrics across different ablated variants. TTFT = Time-to-First-Token, TPOT = Time-Per-Output-Token, QPM = Queries-Per-Minute, E2E = End-to-End latency, OTT = Output Token Throughput, TTT = Total Token Throughput.

Method	TTFT(s)	p99 TTFT(s)	TPOT(ms)	p99 TPOT(ms)	QPM(r/s)	E2E(s)	p99 E2E(s)	OTT(tok/s)	TTT(tok/s)
OmniInfer	2.292	4.198	48	50	616	59.206	148.364	60,575	225,546
w/o OmniPlacement	1.342	2.419	65	68	463	78.025	196.226	45,372	169,083
w/o OmniAttn	1.237	2.174	55	57	554	65.791	161.141	54,533	202,628
w/o OmniProxy	3.683	10.711	50	61	575	63.451	157.843	56,969	211,279
w/o all	1.224	3.374	75	101	404	88.169	213.846	39,954	149,500

- *Batch size scaling.* Larger batch sizes initially improve throughput, but beyond a saturation point TTFT grows disproportionately, indicating the presence of an optimal batching window.
- *Effect of P/D ratio.* The ratio between prefill and decode nodes strongly affects TTFT: higher decode capacity requires additional prefill nodes to maintain balanced utilization and meet SLOs.
- *Scaling inefficiency.* Increasing prefill or decode nodes alone does not scale QPM linearly. For example, 8P8-1D64 provides only marginal gains over 4P8-1D32 despite doubling resources.
- *Data-parallel size.* Larger decode-side data parallelism reduces TPOT but exhibits diminishing returns, consistent with the system-wide throughput saturation trend.

End-to-End Performance Results We perform the final performance evaluation of our system using the best-performing configuration identified in the scaling experiments, namely 6P8-1D32. All proposed components are integrated in this setting, and we further perform an ablation study to quantify the individual contributions of each module. Table 2 presents the tail-latency, throughput, and efficiency metrics across different ablation variants. Several key observations can be drawn:

- *Overall improvement.* The baseline system (w/o all) reaches only 404 QPM, whereas the full OmniInfer configuration achieves 616 QPM—representing a **52%** increase in end-to-end throughput.
- *Impact of sparse-computing modules.* Removing OmniPlacement or OmniAttn reduces throughput to 463 and 554 QPM, respectively. These modules address MoE and attention sparsity, and their removal leads to inefficient batching and increased token generation cost. Quantitatively, they contribute approximately 33% and 11% throughput gains.
- *TPOT-TTFT trade-off at high throughput.* Higher throughput increases the prefill-side pressure and raises

TTFT. For instance, TTFT grows from 1.342 s (w/o OmniPlacement) and 1.237 s (w/o OmniAttn) to 3.683 s when OmniProxy is disabled.

- *Role of OmniProxy as the balancing layer.* With OmniProxy, the system increases throughput from 575 (w/o OmniProxy²) to 616 QPM, while preventing excessive TTFT growth. This highlights OmniProxy’s role as a global scheduler that harmonizes prefill and decode and ensures both efficiency and responsiveness.

Accuracy Results To evaluate the impact of KV-cache compression on model quality, we assess the accuracy of OmniAttn across five representative reasoning benchmarks: AIME24 (AIME, 2024), MMLU-Pro (Wang et al., 2024), GSM8K (Cobbe et al., 2021), LongBench-V2 (Bai et al., 2025), and MATH500 (Hendrycks et al., 2021). Our implementation of OmniAttn accelerates inference by retaining only critical tokens (i.e., attention sinks and recent tokens), thereby reducing the size of the KV cache without modifying model weights. Table 3 summarizes the evaluation results. Across all benchmarks, OmniAttn achieves comparable accuracy relative to the baseline model, demonstrating that KV compression does not lead to significant degradation in reasoning performance. These results indicate that sparse attention patterns can be exploited to improve efficiency while maintaining accuracy, making OmniAttn a practical optimization for large-scale inference.

Table 3. Accuracy comparison between the baseline model and OmniAttn across five reasoning benchmarks.

Method	AIME24	MMLU-Pro	GSM8K	LongBench-V2	MATH500
DS-R1	79.80	84.00	71.50	40.80	87.20
+ OmniAttn	80.28	84.38	69.19	41.90	87.80

7 CONCLUSION AND FUTURE WORK

This paper presented OmniInfer, a unified and hardware co-designed modular system for efficient serving of large language models. By abandoning the monolithic paradigm

²We use the default round-robin load balancer in Nginx when disabling OmniProxy.

in favor of a globally coordinated, disaggregated architecture, OmniInfer flexibly resolves the fundamental tension between prefill and decode computation. Its synergistic components—OmniPlacement for MoE expert scheduling, OmniAttn for sparse attention acceleration, and OmniProxy for global disaggregation-aware scheduling—work in concert to deliver state-of-the-art performance on Ascend NPU hardware. Our extensive evaluation demonstrates substantial improvements in throughput and latency, validating our holistic approach and offering a robust path forward for the next generation of LLM serving infrastructure.

While OmniInfer demonstrates significant performance gains, several directions remain for future work. First, extending support to a broader range of LLMs, acceleration techniques, and multimodal models to further generalize the system. Second, integrating OmniInfer into additional inference frameworks beyond vLLM, leveraging its modular design to facilitate seamless deployment and improvement. Third, adapting OmniInfer to other hardware platforms beyond Ascend NPUs, enabling wider applicability and cross-platform acceleration.

REFERENCES

- Achiam, J., Adler, S., Agarwal, S., Ahmad, L., Akkaya, I., Aleman, F. L., Almeida, D., Altenschmidt, J., Altman, S., Anadkat, S., et al. GPT-4 technical report. *arXiv preprint arXiv:2303.08774*, 2023.
- Agarwal, S., Ahmad, L., Ai, J., Altman, S., Applebaum, A., Arbus, E., Arora, R. K., Bai, Y., Baker, B., Bao, H., et al. gpt-oss-120b & gpt-oss-20b model card. *arXiv preprint arXiv:2508.10925*, 2025.
- Agrawal, A., Kedia, N., Panwar, A., Mohan, J., Kwatra, N., Gulavani, B., Tumanov, A., and Ramjee, R. Taming {Throughput-Latency} tradeoff in {LLM} inference with {Sarathi-Serve}. In *18th USENIX Symposium on Operating Systems Design and Implementation (OSDI 24)*, pp. 117–134, 2024.
- AIME. American invitational mathematics examination - AIME 2024, February 2024. URL <https://maa.org/math-competitions/american-invitational-mathematics-examination-aime>.
- Bai, Y., Tu, S., Zhang, J., Peng, H., Wang, X., Lv, X., Cao, S., Xu, J., Hou, L., Dong, Y., et al. Longbench v2: Towards deeper understanding and reasoning on realistic long-context multitasks. In *Proceedings of the 63rd Annual Meeting of the Association for Computational Linguistics (Volume 1: Long Papers)*, pp. 3639–3664, 2025.
- Cobbe, K., Kosaraju, V., Bavarian, M., Chen, M., Jun, H., Kaiser, L., Plappert, M., Tworek, J., Hilton, J., Nakano, R., et al. Training verifiers to solve math word problems. *arXiv preprint arXiv:2110.14168*, 2021.
- Fedus, W., Zoph, B., and Shazeer, N. Switch transformers: Scaling to trillion parameter models with simple and efficient sparsity. *Journal of Machine Learning Research*, 23(120):1–39, 2022.
- Fu, Y., Zhu, S., Su, R., Qiao, A., Stoica, I., and Zhang, H. Efficient LLM scheduling by learning to rank. In *The Thirty-eighth Annual Conference on Neural Information Processing Systems*, 2024. URL <https://openreview.net/forum?id=wLLjY10Gi6>.
- Guo, D., Yang, D., Zhang, H., Song, J., Wang, P., Zhu, Q., Xu, R., Zhang, R., Ma, S., Bi, X., et al. Deepseek-r1 incentivizes reasoning in LLMs through reinforcement learning. *Nature*, 645(8081):633–638, 2025a.
- Guo, Y., Cheng, Z., Tang, X., Tu, Z., and Lin, T. Dynamic mixture of experts: An auto-tuning approach for efficient transformer models. In *The Thirteenth International Conference on Learning Representations*, 2025b. URL <https://openreview.net/forum?id=T26f9z2rEe>.
- Hendrycks, D., Burns, C., Kadavath, S., Arora, A., Basart, S., Tang, E., Song, D., and Steinhardt, J. Measuring mathematical problem solving with the math dataset. *arXiv preprint arXiv:2103.03874*, 2021.
- Hu, C., Huang, H., Hu, J., Xu, J., Chen, X., Xie, T., Wang, C., Wang, S., Bao, Y., Sun, N., et al. Memserve: Context caching for disaggregated LLM serving with elastic memory pool. *arXiv preprint arXiv:2406.17565*, 2024.
- Hwang, C., Cui, W., Xiong, Y., Yang, Z., Liu, Z., Hu, H., Wang, Z., Salas, R., Jose, J., Ram, P., et al. Tutel: Adaptive mixture-of-experts at scale. *Proceedings of Machine Learning and Systems*, 5:269–287, 2023.
- Ji, T., Guo, B., Wu, Y., Guo, Q., Shen, L., Chen, Z., Qiu, X., Zhang, Q., and Gui, T. Towards economical inference: Enabling deepseek’s multi-head latent attention in any transformer-based llms. *arXiv preprint arXiv:2502.14837*, 2025.
- Jin, Y., Wang, T., Lin, H., Song, M., Li, P., Ma, Y., Shan, Y., Yuan, Z., Li, C., Sun, Y., Wu, T., Chu, X., Huan, R., Ma, L., You, X., Zhou, W., Ye, Y., Liu, W., Xu, X., Zhang, Y., Dong, T., Zhu, J., Wang, Z., Ju, X., Song, J., Cheng, H., Li, X., Ding, J., Guo, H., and Zhang, Z. P/D-Serve: Serving disaggregated large language models at scale. *arXiv preprint*, 2024. URL <https://arxiv.org/abs/2408.08147>.

- Kwon, W., Li, Z., Zhuang, S., Sheng, Y., Zheng, L., Yu, C. H., Gonzalez, J., Zhang, H., and Stoica, I. Efficient memory management for large language model serving with pagedattention. In *Proceedings of the 29th symposium on operating systems principles*, pp. 611–626, 2023.
- Li, Y., Huang, Y., Yang, B., Venkitesh, B., Locatelli, A., Ye, H., Cai, T., Lewis, P., and Chen, D. SnapKV: LLM knows what you are looking for before generation. In *Advances in Neural Information Processing Systems*, volume 37, pp. 22947–22970. Curran Associates, Inc., 2024.
- Liu, A., Feng, B., Wang, B., Wang, B., Liu, B., Zhao, C., Deng, C., Ruan, C., Dai, D., Guo, D., et al. Deepseek-v2: A strong, economical, and efficient mixture-of-experts language model. *arXiv preprint arXiv:2405.04434*, 2024a.
- Liu, A., Feng, B., Xue, B., Wang, B., Wu, B., Lu, C., Zhao, C., Deng, C., Zhang, C., Ruan, C., et al. DeepSeek-V3 technical report. *arXiv preprint arXiv:2412.19437*, 2024b.
- Pan, J. and Li, G. A survey of LLM inference systems. *arXiv preprint arXiv:2506.21901*, 2025.
- Patel, P., Choukse, E., Zhang, C., Shah, A., Goiri, Í., Maleki, S., and Bianchini, R. Splitwise: Efficient generative LLM inference using phase splitting. In *2024 ACM/IEEE 51st Annual International Symposium on Computer Architecture (ISCA)*, pp. 118–132. IEEE, 2024.
- Qin, R., Li, Z., He, W., Zhang, M., Wu, Y., Zheng, W., and Xu, X. Mooncake: A KVCache-centric disaggregated architecture for LLM serving. In *USENIX Conference on File and Storage Technologies (FAST ’25)*, pp. 155–170. USENIX Association, 2025. URL <https://arxiv.org/abs/2407.00079>.
- Rajbhandari, S., Li, C., Yao, Z., Zhang, M., Aminabadi, R. Y., Awan, A. A., Rasley, J., and He, Y. DeepSpeed-MoE: Advancing mixture-of-experts inference and training to power next-generation AI scale. In *International Conference on Machine Learning*, pp. 18332–18346. PMLR, 2022.
- Schick, T., Dwivedi-Yu, J., Dessì, R., Raileanu, R., Lomeli, M., Hambro, E., Zettlemoyer, L., Cancedda, N., and Scialom, T. Toolformer: Language models can teach themselves to use tools. In *Advances in Neural Information Processing Systems*, volume 36, pp. 68539–68551, 2023.
- Sharon, D. and Brichtova, N. Image editing in gemini just got a major upgrade. Blog post, Google Products – Gemini, August 2025. Available at <https://blog.google/products/gemini/updated-image-editing-model/>.
- Singh, G., Wang, X., Hu, Y., Yu, T. T. L., Xing, L., Jiang, W., Wang, Z., Xiaolong, B., Li, Y., Xiong, Y., Zhang, Y., and Fan, Z. Efficiently serving large multimodal models using EPD disaggregation. In *Forty-second International Conference on Machine Learning*, 2025. URL <https://openreview.net/forum?id=n7VLFYN0Cb>.
- Srivatsa, V., He, Z., Abhyankar, R., Li, D., and Zhang, Y. Preble: Efficient distributed prompt scheduling for LLM serving. In *The Thirteenth International Conference on Learning Representations*, 2025. URL <https://openreview.net/forum?id=meKEKDhdxn>.
- Stojkovic, J., Zhang, C., Goiri, Í., Torrellas, J., and Choukse, E. Dynamollm: Designing LLM inference clusters for performance and energy efficiency. In *2025 IEEE International Symposium on High Performance Computer Architecture (HPCA)*, pp. 1348–1362. IEEE, 2025.
- Strati, F., Mcallister, S., Phanishayee, A., Tarnawski, J., and Klimovic, A. DéjàVu: KV-cache streaming for fast, fault-tolerant generative LLM serving. In *Forty-first International Conference on Machine Learning*, pp. 46745–46771. PMLR, 2024.
- Team, K., Bai, Y., Bao, Y., Chen, G., Chen, J., Chen, N., Chen, R., Chen, Y., Chen, Y., Chen, Y., et al. Kimi k2: Open agentic intelligence. *arXiv preprint arXiv:2507.20534*, 2025.
- vLLM Contributors. *Automatic Prefix Caching in vLLM*. vLLM Project, 2025. URL https://docs.vllm.ai/en/latest/features/automatic_prefix_caching.html. Version 0.5.5, accessed November 2025.
- Wang, Y., Ma, X., Zhang, G., Ni, Y., Chandra, A., Guo, S., Ren, W., Arulraj, A., He, X., Jiang, Z., et al. Mmlu-pro: A more robust and challenging multi-task language understanding benchmark. *Advances in Neural Information Processing Systems*, 37:95266–95290, 2024.
- Xiao, G., Tian, Y., Chen, B., Han, S., and Lewis, M. Efficient streaming language models with attention sinks. In *The Twelfth International Conference on Learning Representations*, 2024. URL <https://openreview.net/forum?id=NG7sS51zVF>.
- Xiao, G., Tang, J., Zuo, J., Guo, J., Yang, S., Tang, H., Fu, Y., and Han, S. DuoAttention: Efficient long-context LLM inference with retrieval and streaming heads. In *The Thirteenth International Conference on Learning Representations*, 2025.

- Yang, A., Li, A., Yang, B., Zhang, B., Hui, B., Zheng, B., Yu, B., Gao, C., Huang, C., Lv, C., et al. Qwen3 technical report. *arXiv preprint arXiv:2505.09388*, 2025.
- Yue, T., Guo, L., Cheng, J., Gao, X., Huang, H., and Liu, J. Ada-K Routing: Boosting the efficiency of moe-based LLMs. In *The Thirteenth International Conference on Learning Representations*, 2025. URL <https://openreview.net/forum?id=9CqkpQExe2>.
- Zhang, Z., Sheng, Y., Zhou, T., Chen, T., Zheng, L., Cai, R., Song, Z., Tian, Y., Ré, C., Barrett, C., Wang, Z. A., and Chen, B. H2O: Heavy-hitter oracle for efficient generative inference of large language models. In *Advances in Neural Information Processing Systems*, volume 36, pp. 34661–34710. Curran Associates, Inc., 2023.
- Zheng, L., Yin, L., Xie, Z., Sun, C. L., Huang, J., Yu, C. H., Cao, S., Kozyrakis, C., Stoica, I., Gonzalez, J. E., et al. SGLang: Efficient execution of structured language model programs. In *Advances in Neural Information Processing Systems*, volume 37, pp. 62557–62583, 2024.
- Zhong, Y., Liu, S., Chen, J., Hu, J., Zhu, Y., Liu, X., Jin, X., and Zhang, H. DistServe: Disaggregating prefill and decoding for goodput-optimized large language model serving. In *18th USENIX Symposium on Operating Systems Design and Implementation (OSDI 24)*, pp. 193–210, 2024.
- Zhou, Y., Lei, T., Liu, H., Du, N., Huang, Y., Zhao, V., Dai, A. M., Le, Q. V., Laudon, J., et al. Mixture-of-experts with expert choice routing. In *Advances in Neural Information Processing Systems*, volume 35, pp. 7103–7114, 2022.
- Zhou, Z., Ning, X., Hong, K., Fu, T., Xu, J., Li, S., Lou, Y., Wang, L., Yuan, Z., Li, X., et al. A survey on efficient inference for large language models. *arXiv preprint arXiv:2404.14294*, 2024.
- ZillizTech. DeepSearcher: Open source deep research alternative to reason and search on private data. <https://github.com/zilliztech/deep-searcher>, 2025. Apache-2.0, starred 6.9k.
- Zuo, P., Lin, H., Deng, J., Zou, N., Yang, X., Diao, Y., Gao, W., Xu, K., Chen, Z., Lu, S., et al. Serving large language models on Huawei CloudMatrix384. *arXiv preprint arXiv:2506.12708*, 2025.